

Valve-based compensation for controllability improvement of the energy-saving electrohydraulic flow matching system*

Min CHENG^{†1,2}, Bing XU², Jun-hui ZHANG², Ru-qi DING^{2,3}

(¹State Key Laboratory of Mechanical Transmissions, School of Mechanical Engineering, Chongqing University, Chongqing 400044, China)

(²State Key Laboratory of Fluid Power and Mechatronic Systems, Zhejiang University, Hangzhou 310027, China)

(³School of Mechatronic Engineering, East China Jiaotong University, Nanchang 330013, China)

[†]E-mail: chengmin@cqu.edu.cn

Received Apr. 29, 2016; Revision accepted Oct. 21, 2016; Crosschecked May 15, 2017

Abstract: The energy-saving electrohydraulic flow matching (EFM) system opens up an opportunity to minimize valve losses by fully opening the control valves, but the controllability is lost under overrunning load conditions. To address this issue, this paper proposes a valve-based compensator to improve the controllability of the energy-saving EFM system. The valve-based compensator consists of a static compensator and a differential dynamic compensator based on load conditions. The energy efficiency, the stability performance, and the damping characteristic are analyzed under different control parameters. A parameter selection method is used to improve the efficiency, ensure the stability performance, and obtain good dynamic behavior. A test rig with a 2-t hydraulic excavator is built, and experimental tests are carried out to validate the proposed valve-based compensator. The experimental results indicate that the controllability of the EFM system is improved, and the characteristic of high energy efficiency is obtained by the proposed compensator.

Key words: Compensation control; Energy efficient; Flow matching; Mobile machinery

<http://dx.doi.org/10.1631/jzus.A1600346>

CLC number: TH137.1


1 Introduction

The hydraulic system is one of the most important transmission systems in mobile machinery such as excavators (Lin *et al.*, 2008), vehicles (Ekoru and Pedro, 2013), and robots (Yang and Pan, 2015). The valve-controlled hydraulic system has found widespread application in mobile machinery due to its satisfying response and dynamic behavior. However, pressure losses of control valves are still significant so

that the energy efficiency is extremely low (ranging from 6% to 40%). For instance, typical digging cycles of hydraulic excavators show that over 40% of the hydraulic energy is lost by control valves with no possibility of recovery (Stelson, 2011). Therefore, although good controllability can be obtained in valve-controlled systems, the energy efficiency needs to be further improved to help cope with energy crisis and environmental pollution.

In the past few decades, many approaches have been proposed to improve the energy efficiency by eliminating or reducing valve losses. One of the energy efficient alternatives is the displacement controlled system, in which the hydraulic actuators are controlled directly by variable displacement pumps (Daher and Ivantysynova, 2015), so valve losses are completely eliminated. However, it leads to challenging controller design owing to hard nonlinearities

* Project supported by the National Natural Science Foundation of China (No. 51375431), the Open Fund of the State Key Laboratory of Fluid Power and Mechatronic Systems (No. GZKF-201503), and the Research Fund of the State Key Laboratory of Mechanical Transmission (No. SKLMT-ZZKT-2015Z10), China

 ORCID: Min CHENG, <http://orcid.org/0000-0002-8345-6657>

© Zhejiang University and Springer-Verlag Berlin Heidelberg 2017

and high-order dynamic characteristics (Wang and Wang, 2014). In addition, the hydraulic actuators can be driven directly by variable-speed fixed displacement pumps (Minav *et al.*, 2013), but their application is limited in mobile machinery since hydraulic systems are often powered by and mechanically coupled to an internal combustion engine (Heybroek, 2008). Another approach is to replace traditional control valves by hydraulic transformers, so the pump pressure could be transformed to the load pressure, and then the hydraulic power is merely lost (Inderelst *et al.*, 2010). A transformer design with high efficiency, high bandwidth, low noise, and acceptable cost has not yet been achieved (Ketonen *et al.*, 2010). An alternative method is to use digital hydraulic valves instead of traditional proportional valves (Laamanen and Vilenius, 2003). Digital control valves are rapidly fully opened and closed in working conditions, so valve losses are eliminated, at least in theory (Linjama, 2011). Based on the digital hydraulic concept, lots of energy-saving components have been proposed, such as digital pumps/motors (Merrill *et al.*, 2010), hydraulic switching converters (Kogler and Scheidl, 2008), and digital hydraulic power management systems (Heikkilä and Linjama, 2013). However, there are still many challenges that hinder the mass application of digital hydraulics, e.g., noise and pressure pulsation (Linjama, 2011).

From the aforementioned reviews, it is seen that further improvements have to be made before these promising hydraulic components or circuits are applied in mobile machinery. Recently, the electrohydraulic flow matching (EFM) concept opens up an opportunity to improve the energy efficiency with just small modifications to the existing valve-controlled systems (Mettälä *et al.*, 2007; Axin, 2013; Borghi *et al.*, 2014). In EFM systems, pump flow rates are directly controlled by input devices (e.g., joysticks), so the energy efficient method by fully opening the control valve was proposed to minimize valve losses (Finzel and Helduser, 2008; Axin *et al.*, 2014; Xu *et al.*, 2015b; 2015c; Du *et al.*, 2016). However, if the meter-out orifice is maximized, the hydraulic cylinder makes an overspeed movement in the case of pulling loads (Finzel and Helduser, 2008). Therefore, this method of fully opening the valve fails in the over-running load condition, which is a significant drawback for the controllability of mobile machinery.

To improve the energy efficiency and ensure controllability, in this study, we discuss how to improve the system controllability by managing the valve opening based on load conditions. A valve compensation controller is proposed, consisting of static and dynamic compensators. In this paper, the system principle and the mathematical model are introduced first. Then, the proposed controller is described, and the efficiency, the stability, and the dynamic behavior are analyzed. At last, the test rig and the experimental results are shown.

2 System modeling

A typical electrohydraulic system for mobile machinery is shown in Fig. 1. It consists of a prime mover, an electronically controlled pump, a relief valve, a primary pressure compensator, a proportional control valve, and a hydraulic cylinder. The control valve is composed of two coupled orifices, the meter-in orifice and the meter-out orifice.

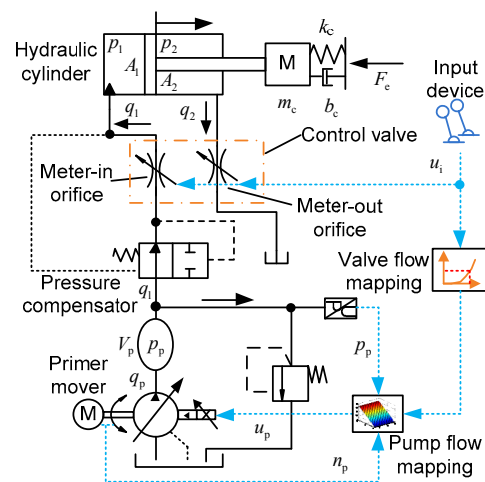


Fig. 1 Schematic diagram of a typical electrohydraulic control system for mobile machinery (the variables will be explained in the text)

According to the EFM concept (Finzel and Helduser, 2008), both the pump displacement and the valve opening are controlled simultaneously by the input device. The pump displacement is calculated from the required flow rate that only depends on the valve opening. The pressure drop of the meter-in

orifice is limited by the pressure compensator, so the required flow rate of the control valve can be expressed as

$$q_1 = C_d A(x_v) \sqrt{\frac{2\Delta p_m}{\rho}}, \quad (1)$$

where q_1 is the flow rate across the meter-in orifice, x_v the valve opening, $A(x_v)$ the cross-sectional area, C_d the flow coefficient, and ρ the oil density. The specific pressure drop Δp_m can be considered as a constant value if the supplied flow is sufficient. Considering the pump leakage, the supplied flow can be described by

$$q_p = f(u_p, p_p) = n_p k_p u_p - k_{lp} p_p, \quad (2)$$

where q_p is the supplied flow from the pump, u_p the pump control signal, p_p the pump pressure, n_p the rotational speed of the prime mover, k_p the pump gain, and k_{lp} the pump leakage gain. Then the pump control signal can be calculated as

$$u_p = \frac{C_d A(x_v) \sqrt{\frac{2\Delta p_m}{\rho}} + k_{lp} p_p}{n_p k_p}. \quad (3)$$

If the relief valve is closed, the continuous equation of the pipe chamber between the pump and the valve can be expressed as

$$p_p(s) = \frac{\beta_e}{V_p s} [q_p(s) - q_1(s)], \quad (4)$$

where s is the Laplace operator, β_e the effective bulk modulus, and V_p the chamber volume between the pump and valve. Assuming that the pipe chamber between the pump and the valve is small enough, it can be considered that $q_1 = q_p$. The force balance equation of the hydraulic rod can be expressed as

$$\left(m_c s + b_c + \frac{k_c}{s} \right) v_c(s) = A_1 p_1(s) - A_2 p_2(s) - F_e(s), \quad (5)$$

where m_c is the load mass, b_c the load viscous damping, k_c the load stiffness, v_c the cylinder velocity, A_1 the capside area of the cylinder, A_2 the rodside area

of the cylinder, p_1 the capside pressure of the cylinder, p_2 the rodside pressure of the cylinder, and F_e the external load force. The linearization form of the meter-out orifice equation can be written as

$$q_2(s) = k_q x_v(s) + k_{pq} p_2(s), \quad (6)$$

where q_2 is the flow rate across the meter-out orifice, k_q the flow gain of the meter-out orifice, $k_q = C_d W_d \sqrt{2p_{20}/\rho}$, W_d the hydraulic diameter of the meter-out orifice, p_{20} the rodside pressure of the cylinder under the linearization operating point, k_{pq} the flow-pressure gain of the meter-out orifice, $k_{pq} = C_d W_d x_{v0} / \sqrt{p_{20}\rho}$, and x_{v0} the meter-out orifice opening under the linearization point. If the cylinder leakage is neglected, the continuous equation of the capside chamber and the rodside chamber can be written as

$$q_1(s) = q_1(s) = A_1 v_c(s) + \frac{V_1}{\beta_e} s p_1(s), \quad (7)$$

$$q_2(s) = A_2 v_c(s) - \frac{V_2}{\beta_e} s p_2(s), \quad (8)$$

where V_1 is the chamber volume between the cylinder and the meter-in orifice, and V_2 the chamber volume between the cylinder and the meter-out orifice. The cylinder velocity can be drawn from Eqs. (4)–(8) as

$$v_c(s) = \frac{B(s)}{A(s)} q_p(s) + \frac{C(s)}{A(s)} x_v(s) + \frac{D(s)}{A(s)} F_e(s), \quad (9)$$

where

$$\begin{aligned} A(s) = & m_c V_1 V_2 s^3 + (k_{pq} \beta_e m_c V_1 + b_c V_1 V_2) s^2 \\ & + (k_{pq} \beta_e b_c V_1 + A_2^2 V_1 \beta_e + A_1^2 V_2 \beta_e + k_c V_1 V_2) s \\ & + k_{pq} \beta_e (k_c V_1 + A_1^2 \beta_e), \end{aligned} \quad (10)$$

$$B(s) = (V_2 s + k_{pq} \beta_e) A_1 \beta_e, \quad (11)$$

$$C(s) = A_2 V_1 \beta_e k_q s, \quad (12)$$

$$D(s) = -V_1 s (V_2 s + k_{pq} \beta_e). \quad (13)$$

Therefore, the steady-state velocity of the hydraulic cylinder can be written as

$$v_{c-st} = \frac{q_p \beta_e A_1}{A_1^2 \beta_e + k_c V_1}. \quad (14)$$

In the traditional method (subsequently called the traditional controller), the valve control signal directly follows the signal of the input device (e.g., joysticks) by the operators, as shown in Fig. 1. An energy-saving method of fully opening the control valve has been proposed (subsequently called the maximum controller), but it fails in the overrunning load conditions. Thus, a new valve controller is proposed to cope with this issue in the following section.

3 Control strategy and analysis

3.1 Controller design

In the electrohydraulic system shown in Fig. 1, the oil supplied by the pump is fully charged into the cylinder as long as the relief valve is closed. Thus, the steady-state velocity performance remains the same no matter the dimension of the valve opening, which can be also seen from Eq. (14). Therefore, the control valve can be fully opened to reduce its pressure loss and improve system efficiency. However, as mentioned in Section 1, the load velocity could be limited by the meter-out orifice in overrunning load conditions, leading to deterioration of velocity performance (Finzel and Helduser, 2008). For instance, if a pulling load exerting on the rod is too large to be balanced by the resistance force generated by the rodside pressure, the rod will unexpectedly make an overspeed movement. At the same time, the expanding capsid chamber cannot be filled fully by the oil, so the cavitation will occur.

In order to solve this problem, an intuitive solution is to output maximum control signal of the valve (u_m) in resistive conditions ($F_e > 0$) and deliver the input command u_i (control signal from the input device) in overrunning conditions ($F_e < 0$). Then the efficiency improvement and velocity performance can be ensured in resistive and overrunning conditions, respectively. However, the control signal switches between u_m and u_i if the load force F_e fluctuates near zero, leading to oscillations or instabilities. Therefore, a static compensator shown in Fig. 2 is designed and added to adjust the valve opening. A boundary layer is introduced between the two control signals u_m and u_i in the proposed controller. It is defined that $F_l(t)$ is the driving force to actuate the hydraulic rod ($F_l(t) = p_{1p}(t)A_1 - p_{2p}(t)A_2$, where p_{1p} and p_{2p}

are the capsid pressure and the rodside pressure of the cylinder of the proposed controller, respectively).

Then the static compensator is written as

$$u_{vs}(F_l) = \begin{cases} u_m - u_i, & F_l > \phi, \\ \frac{F_l}{\phi}(u_m - u_i), & 0 \leq F_l \leq \phi, \\ 0, & F_l < 0, \end{cases} \quad (15)$$

where ϕ is the static control boundary. Referring to the principle of dynamic pressure feedback (DeBoer and Yao, 2001; Cristofori *et al.*, 2012; Zaev *et al.*, 2013), a dynamic compensator is designed and added into the valve controller to improve the dynamic performance. This is expressed as

$$u_{vd}(F_l) = \begin{cases} k_{vd} [\dot{p}_{1p}(t)A_1 - \dot{p}_{2p}(t)A_2], & 0 \leq F_l \leq \phi, \\ 0, & F_l > \phi \text{ or } F_l < 0, \end{cases} \quad (16)$$

where k_{vd} is the dynamic gain. It is seen that $u_{vd}=0$ in steady-state load conditions. The valve control signal of the proposed controller can be written as

$$u_{vp} = u_i + u_{vs}(F_l) + u_{vd}(F_l). \quad (17)$$

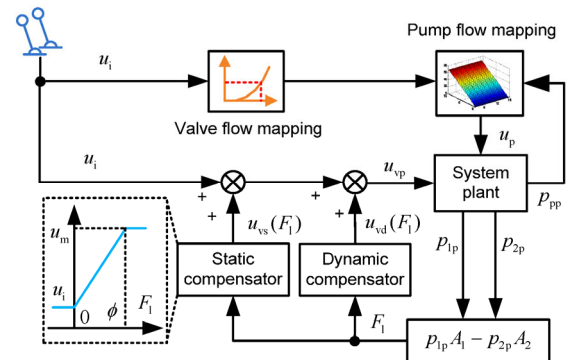


Fig. 2 Schematic diagram of the proposed controller

3.2 Comparison of energy efficiency

This section compares the energy efficiencies of the proposed controller and the traditional controller under steady-state conditions. To analyze the energy-saving characteristic of the proposed controller, the following assumptions are considered reasonable:

1. Neglecting the pilot oil in the pressure compensator, the oil supplied by the pump all flows into the cylinder.

2. The control valve is symmetric, which means that the cross-sectional area of the meter-in orifice is equal to that of the meter-out orifice.

3. The tank pressure is considered as zero, and the cylinder leakage is neglected.

Based on the assumptions above, the electrohydraulic systems by the traditional controller and the proposed controller are simplified as shown in Fig. 3.

Therefore, the following equations, Eqs. (18)–(21), can be drawn from the mathematical model described in Section 2.

$$q_p = C_d A(x_v) \sqrt{\frac{2\Delta p_m}{\rho}} = C_d A(x_{vp}) \sqrt{\frac{2(p_{pp} - p_{1p})}{\rho}}, \quad (18)$$

$$q_2 = C_d A(x_v) \sqrt{\frac{2p_2}{\rho}} = C_d A(x_{vp}) \sqrt{\frac{2p_{2p}}{\rho}}, \quad (19)$$

$$v_c = \frac{q_p}{A_1} = \frac{q_2}{A_2}, \quad (20)$$

$$A_1 p_{1p} - A_2 p_{2p} = A_1 p_1 - A_2 p_2, \quad (21)$$

where x_{vp} and $A(x_{vp})$ are the valve opening and cross-sectional area of the proposed controller, respectively, and p_{pp} is the pump pressure of the proposed controller. The reduced system pressure consists of the reduced pressure in the capside chamber and the reduced pressure drop over the meter-in orifice, which is drawn from Eqs. (18)–(21) as

$$\begin{aligned} \Delta p_p &= p_p - p_{pp} = (p_1 - p_{1p}) + (\Delta p_m - p_{pp} + p_{1p}) \\ &= \frac{A_2}{A_1} (p_2 - p_{2p}) + (\Delta p_m - p_{pp} + p_{1p}) \\ &= \frac{(A_1^3 + A_2^3) [A^2(x_{vp}) - A^2(x_v)]}{A_1^3 A^2(x_{vp})} \Delta p_m. \end{aligned} \quad (22)$$

In contrast to the traditional controller, the energy-saving ratio with the proposed controller can be written as

$$\eta_e = \frac{\Delta p_p}{p_p} = \frac{(A_1^3 + A_2^3) [A^2(x_{vp}) - A^2(x_v)] \Delta p_m}{A_1^3 A^2(x_{vp}) p_p}. \quad (23)$$

Similarly, the energy-saving ratio when the cylinder retracts can be expressed as

$$\eta_r = \frac{(A_1^3 + A_2^3) [A^2(x_{vp}) - A^2(x_v)] \Delta p_m}{A_2^3 A^2(x_{vp}) p_p}. \quad (24)$$

Therefore, the energy-saving ratio depends on the system pressure and the specified pressure drop Δp_m . In addition, the smaller input command u_i results in higher energy efficiency. The energy-saving ratios of the proposed system under different driving forces and static control boundaries are shown in Fig. 4. It is seen that the energy-saving ratio can be improved by reducing ϕ if the load force falls within the range of $[0, \phi]$.

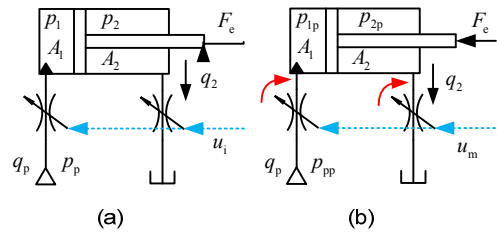


Fig. 3 Simplified systems for the traditional controller (a) and the proposed controller (b)

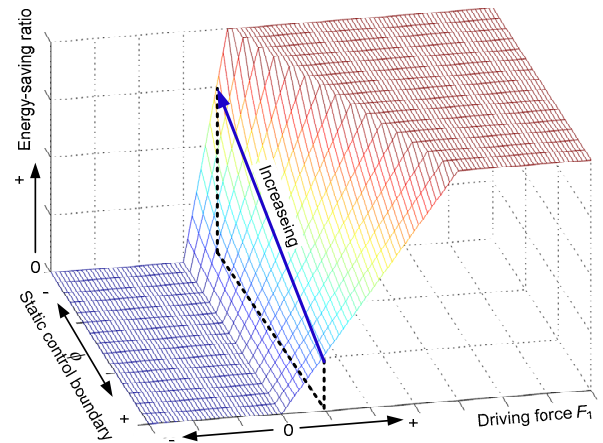


Fig. 4 Energy-saving ratio under different driving forces and static control boundaries

3.3 Analysis of stability performance

When the driving force F_1 varies within the range from 0 to ϕ , the valve is regulated continuously by the proposed controller. If the spool displacement is

proportional to the control signal, x_{vp} is drawn from Eqs. (15)–(17) as

$$x_{vp}(s) = x_i(s) + \frac{F_1(s)}{\phi} [x_{vm} - x_i(s)] + k_{vd}k_v s F_1(s), \quad (25)$$

$$0 \leq F_1 \leq \phi,$$

where x_i is the valve opening under the input command, x_{vm} the maximum valve opening, and k_v the displacement gain of the spool. From Eqs. (9)–(13) and (25), the velocity of the hydraulic cylinder can be written as

$$v_{cp}(s) = \frac{\phi B(s)q_p(s) + \phi C(s)x_i(s)}{N_3 s^3 + N_2 s^2 + N_1 s + N_0} + \frac{[\phi D(s) + C(s)(x_{vm} - x_i) + C(s)\phi k_{vd}k_v s]F_e(s)}{N_3 s^3 + N_2 s^2 + N_1 s + N_0}, \quad (26)$$

where

$$N_3 = \phi m_c V_1 V_2 \left(1 - \frac{k_{vd}k_v A_2 \beta_e k_q}{V_2} \right), \quad (27)$$

$$N_2 = \beta_e m_c V_1 \phi k_{pq} \left[1 - \frac{k_q A_2 (x_{vm} - x_i)}{\phi k_{pq}} \right] + \phi b_c V_1 V_2 \left(1 - \frac{k_{vd}k_v A_2 \beta_e k_q}{V_2} \right), \quad (28)$$

$$N_1 = \phi \beta_e (A_2^2 V_1 + A_1^2 V_2) + \beta_e b_c V_1 \phi k_{pq} \left[1 - \frac{k_q A_2 (x_{vm} - x_i)}{\phi k_{pq}} \right] + \phi k_c V_1 V_2 \left(1 - \frac{k_{vd}k_v A_2 \beta_e k_q}{V_2} \right), \quad (29)$$

$$N_0 = \phi k_{pq} A_1^2 \beta_e^2 + \beta_e k_c V_1 \phi k_{pq} \left[1 - \frac{k_q A_2 (x_{vm} - x_i)}{\phi k_{pq}} \right]. \quad (30)$$

According to the Routh-Hurwitz criteria, the stability condition of Eq. (26) can be given by

$$\begin{cases} N_i > 0, & i = 1, 2, 3, 4, \\ \frac{N_1 N_2 - N_0 N_3}{N_1} > 0, \end{cases} \quad (31)$$

If the control parameters ϕ and k_{vd} are selected so that the following expression

$$\alpha = 1 - \frac{k_q A_2 (x_{vm} - x_i)}{\phi k_{pq}} \geq 1 - \frac{k_{vd} A_2 \beta_e k_q k_v}{V_2} > 0 \quad (32)$$

is satisfied (where $0 \leq \alpha \leq 1$), given that $N_i > 0$ and

$$\begin{aligned} N_1 N_2 - N_0 N_3 &\geq \beta_e m_c V_1 \phi k_{pq} \alpha \\ &\times \left[\phi \beta_e (A_2^2 V_1 + A_1^2 V_2) + \phi k_c V_1 V_2 \left(1 - \frac{k_{vd}k_v A_2 \beta_e k_q}{V_2} \right) \right. \\ &\quad \left. - \phi m_c V_1 V_2 \left(1 - \frac{k_{vd}k_v A_2 \beta_e k_q}{V_2} \right) \right. \\ &\quad \left. \times (\phi k_{pq} A_1^2 \beta_e^2 + \beta_e k_c V_1 \phi k_{pq} \alpha) \right] \\ &= \alpha m_c k_{pq} \beta_e^2 A_2^2 V_1^2 \phi^2 > 0. \end{aligned} \quad (33)$$

Therefore, the stability condition of the proposed controller can be simplified as

$$\phi = \frac{k_q A_2 (x_{vm} - x_i)}{(1 - \alpha) k_{pq}} = \frac{2 p_{20} A_2 (x_{vm} - x_i)}{(1 - \alpha) x_{vp0}}, \quad (34)$$

where x_{vp0} is the valve opening by the proposed controller under the operating point. The system parameters p_{20} , x_{vp0} , x_i , and A_2 are all measureable, so the task is shifted to selecting a proper α to determine ϕ . From the discussion in Section 2, the static boundary ϕ needs to be as small as possible to improve the energy efficiency, so α should be nearly zero to obtain the smallest ϕ . Moreover, Eq. (34) is established according to the linearization model under a specified operating point, so the load condition of the mobile machinery is also involved in determining ϕ in actual application. If the external load of mobile machinery (e.g., excavators) varies violently, a relatively large α should be selected to reduce potential system oscillations. For the machinery with milder load variations (e.g., forklifts), α should be smaller to improve the energy efficiency. The dynamic gain k_{vd} can be deduced from Eq. (32) as

$$\frac{(1 - \alpha) V_2}{A_2 \beta_e k_q k_v} \leq k_{vd} \leq \frac{V_2}{A_2 \beta_e k_q k_v}. \quad (35)$$

The volume V_2 varies under different positions of the hydraulic piston, so displacement sensors must be used for measuring V_2 . However, displacement sensors of hydraulic cylinders are not commonly used in construction machinery due to high cost and low reliability (Garimella and Yao, 2002). It is satisfied that $V_{20} \leq V_2 \leq V_{20} + l_c A_2$, where V_{20} is the minimum value of V_2 under different positions of the hydraulic rod, and l_c the stroke of the hydraulic cylinder. The dynamic gain k_{vd} is selected based on the following Eq. (36) to ensure the universality of the proposed controller.

$$k_{vd} = \gamma \frac{V_{20}}{A_2 \beta_e k_q k_v} = \gamma \frac{V_{20}}{A_2 \beta_e C_d W_d k_v} \sqrt{\frac{2 \Delta p_{20}}{\rho}}, \quad (36)$$

$$\frac{(1-\alpha)(V_{20} + A_2 l_c)}{V_{20}} < \gamma \leq 1,$$

where γ is the dynamic coefficient. The nominal flow of the meter-out orifice is written as

$$Q_{nom} = C_d W_d k_v u_m \sqrt{\frac{2 \Delta p_{nom}}{\rho}}, \quad (37)$$

where Δp_{nom} and Q_{nom} are the nominal pressure drop and flow rate across the meter-out orifice under the maximum valve signal, respectively. Therefore, Eq. (36) can be rewritten as

$$k_{vd} = \gamma \frac{V_{20} u_m}{A_2 \beta_e Q_{nom}} \sqrt{\frac{p_{20}}{\Delta p_{nom}}}, \quad (38)$$

$$\frac{(1-\alpha)(V_{20} + A_2 l_c)}{V_{20}} < \gamma \leq 1.$$

The determination of γ is highly related to the dynamic performance of the hydraulic system, which is discussed in the following section.

3.4 Analysis of static and dynamic behavior

In this section, the steady-state velocity, the damping performance, and the natural frequency are analyzed to compare with the controllability of the proposed controller and the maximum controller. Based on Eq. (26), the steady-state velocity by the proposed controller is expressed as

$$v_{cp-st} = \begin{cases} \frac{q_p \beta_e A_1}{A_1^2 \beta_e + k_c V_1}, & F_1 > \phi \text{ or } F_1 < 0, \\ \frac{q_p \beta_e A_1}{A_1^2 \beta_e + \alpha k_c V_1}, & 0 \leq F_1 \leq \phi. \end{cases} \quad (39)$$

The cylinder velocity is larger when $F_1 \in [0, \phi]$, which is equivalent to that under another stiffness $k_c' = \alpha k_c$. Actually, the load stiffness k_c itself is time-variant and much smaller than $A_1^2 \beta_e / V_1$ in most applications. Therefore, it is considered that the system with the proposed controller is controllable by the operators. To analyze the dynamic behavior, the transfer function from the supplied flow to the velocity by the maximum controller is expressed as

$$\frac{v_c(s)}{q_p(s)} = \frac{(V_2 s + k_{pq} \beta_e) A_1 \beta_e}{A(s)}. \quad (40)$$

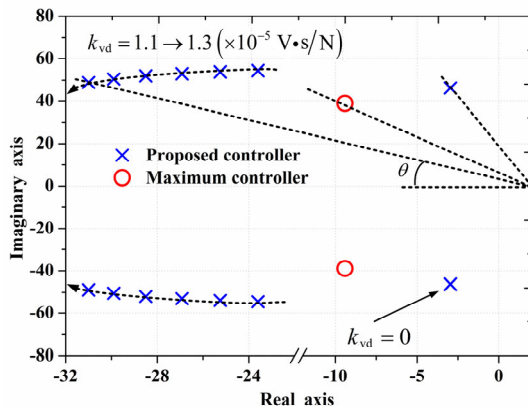
The transfer function from the supplied flow to the velocity by the proposed controller can be expressed as

$$\frac{v_c(s)}{q_p(s)} = \frac{(V_2 s + k_{pq} \beta_e) A_1 \beta_e}{N_3 s^3 + N_2 s^2 + N_1 s + N_0}. \quad (41)$$

The dynamic compensator $u_{vd}(F_1)$ is introduced to improve the dynamic behavior. Using Eqs. (40) and (41) and the parameters in Table 1, the effects of the dynamic compensator are illustrated in Figs. 5 and 6. The pole locations under different dynamic gains are calculated and shown in Fig. 5. It is found that if $k_{vd} = 0$ (the dynamic compensator is not active), the system damping ζ_h ($\zeta_h = \cos \theta$, and θ is the angle of the horizontal axis and connecting line between the origin and pole) by the proposed controller is smaller than that of the traditional controller. As the dynamic gain k_{vd} increases, the system damping increases gradually so that the dynamic behavior is improved. Selecting $k_{vd} = 1.3 \times 10^{-5} \text{ V} \cdot \text{s/N}$, the Bode diagrams with the proposed controller and the maximum controller are illustrated in Fig. 6. It is found that the bandwidth frequency of the system with the maximum controller is 9.2 Hz, and the bandwidth frequency with the proposed controller is 13.5 Hz. Thus, the bandwidth frequency is improved by 4.3 Hz by the proposed controller.

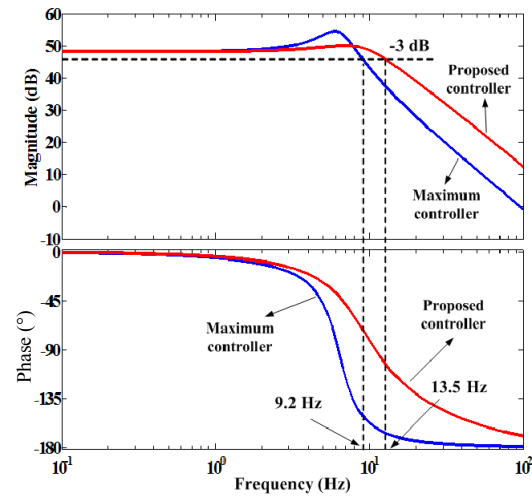
Table 1 Parameters for pole determination (Liu, 2011; Wang and Wang, 2014)

Parameter	Value
Effective bulk modulus, β_e (MPa)	7.0×10^2
Maximum valve opening, x_{vm} (m)	6.0×10^{-3}
Valve opening under the input command, x_i (m)	3.3×10^{-3}
Flow gain of the meter-out orifice, k_q (m^2/s)	0.1
Flow-pressure gain of the meter-out orifice, k_{pq} ($m^3/(s \cdot Pa)$)	1.4×10^{-10}
Load mass, m_c (kg)	5.0×10^3
Load viscous damping, b_c (N·s/m)	5.0×10^4
Load stiffness, k_c (N/m)	1.0×10^4
Acting area of the capsicle chamber, A_1 (m^2)	3.85×10^{-3}
Volume of the capsicle chamber, V_1 (m^3)	1.5×10^{-3}
Acting area of the rodside chamber, A_2 (m^2)	2.59×10^{-3}
Volume of the rodside chamber, V_2 (m^3)	1.5×10^{-3}

**Fig. 5** Pole locations of the system with the proposed controller and the maximum controller

Therefore, the damping performance and the bandwidth frequency are both improved by introducing the dynamic compensator. From the denominator of the transfer function, Eq. (26), it is seen that if the system parameters are all known or measurable, the parameters γ and k_{vd} can be selected accordingly so that the optimized damping $\zeta_{h-opt}=0.707$ (Kim *et al.*, 2012) is obtained. Unfortunately, the system parameters m_c , b_c , and k_c are all time-variant and difficult to measure in most mobile machinery. Considering the time-varying load conditions and system

uncertainties, an experiment-based method is adopted as an alternative to determine γ . Based on Eq. (38), experimental tests with different values of γ are carried out under typical load conditions first, and then the dynamic behavior of the hydraulic cylinder is evaluated and compared. In this way, the dynamic coefficient γ is determined so that satisfying damping and response performance can be obtained under typical load conditions.

**Fig. 6** Bode diagrams of the system with the proposed controller and the maximum controller

4 Experimental study

4.1 Test rig

A test rig with a 2-t hydraulic excavator was used to validate the proposed controller experimentally. The excavator was equipped with an electronically controlled pump from Bosch Rexroth, Germany and a proportional multi-way valve from Danfoss, Denmark. The system parameters are listed in Table 2. The arm cylinder with a broad load variation range was selected as the control object. The photograph of the test rig is shown in Fig. 7. The spool of the control valve locates at the central position, the negative maximum position, and the positive maximum position under the control signal of 6 V, 3 V, and 9 V, respectively. Pressure transducers and velocity sensors were used to provide feedback and monitor the system state, respectively. A flow meter was mounted into the hydraulic circuit to identify the flow mapping of the pump and the valve. A PCI 6229

data acquisition card from National Instrument, USA was used to collect the sensor signals and deliver the control signals. Low pass filters were used to filter the interference noise. The control algorithms were carried out on the MATLAB xPC Target real-time system with a sampling time of 0.5 ms. The static flow mappings of the valve and the pump were identified experimentally, and the detailed results can be found in authors' previous study (Xu *et al.*, 2015a; 2016).

Table 2 Main parameters of the test rig

Parameter	Value
Maximum displacement of the pump (ml/r)	45.6
Rotational speed of the motor (r/min)	1000
Preset pressure of the relief valve (MPa)	13
Diameter of the arm cylinder (m)	0.07
Rod diameter of the arm cylinder (m)	0.04
Stroke of the arm cylinder (m)	0.376

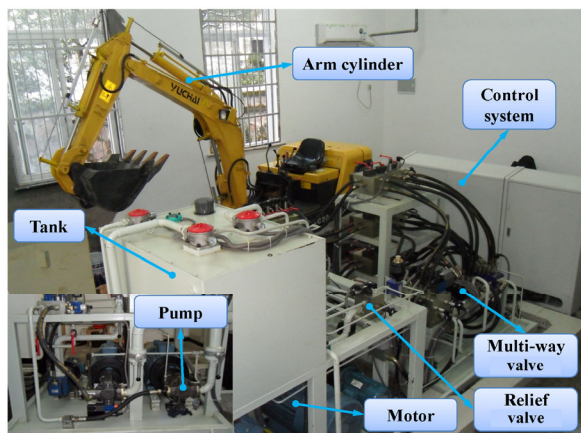


Fig. 7 Test rig with the 2-t hydraulic excavator

4.2 Experimental results

First, tests with different values of α and γ were conducted based on Eqs. (34) and (38) under typical working conditions, and then the optimized values of α and γ in the proposed controller were determined as 0.8 and 0.65, respectively. Then, tests of the arm cylinder were carried out with the three controllers: the traditional controller, the proposed controller, and the maximum controller (the valve is fully opened). The initial positions of the arm cylinder were the same in the tests. Constant input commands were generated from the control system, and then the con-

trol signals were delivered to the valve by the three controllers.

The comparison among the valve signals is shown in Fig. 8a. The 7.5 V and 9 V signals are delivered by the traditional controller and the maximum controller from 10 s, respectively. The cylinder extends until it reaches the end stop. From the load force depicted in Fig. 8b, it is seen that the cylinder is exerted by an overrunning load first and then a resistive load. The control signal from the proposed controller is continuously adjusted, which is maintained at 7.5 V first and then gradually increases to 9 V. The comparison of the load velocity is shown in Fig. 9. At the beginning, the load velocity depends on the overrunning load force and the opening of the meter-out orifice, which is not related to the supplied flow of the pump. The cylinder with the maximum controller runs in an overspeed extending mode under the overrunning load condition, so the load velocity is significantly different from that of the traditional controller unless the cylinder is exerted by a resistive load. While the valve opening is adaptively regulated by the proposed controller according to the load force, the load velocity is matched with that of the traditional controller under the overall load conditions. Additionally, it can be seen that no instability occurs by the proposed controller.

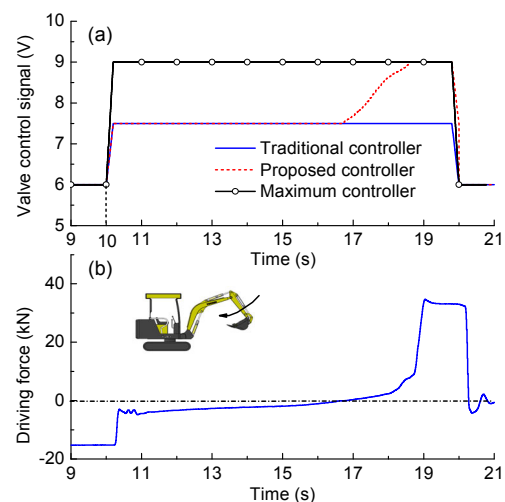


Fig. 8 Comparison of the valve control signals and the load force under the constant input commands

As shown in Fig. 10, the system pressure of the maximum controller is reduced in comparison to that of the traditional controller under the overall motion

process. The system pressure of the proposed controller is reduced after almost 17 s when the load force is above zero. Note that the system pressure of the proposed controller is lower than that of the maximum controller at the same moment (e.g., the pressure at 18 s), although the control signals are both at the maximum values. The reason for this is that the arm cylinder locates at different positions at the same moment, which leads to different external loads and pump pressures.

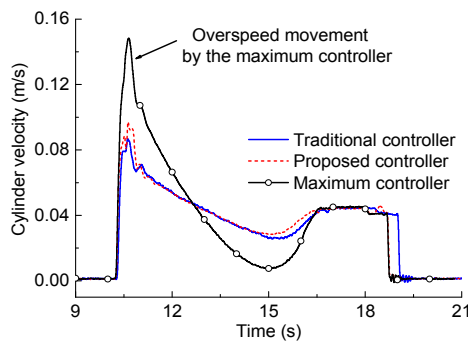


Fig. 9 Load velocity comparison under the constant input commands

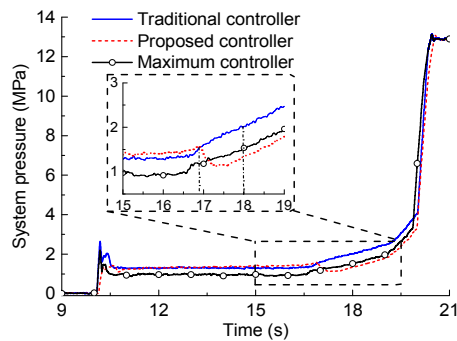


Fig. 10 System pressure comparison under the constant input commands

To evaluate the energy characteristic of the hydraulic system, the energy consumption and the effective efficiency are defined as follows (Troxel and Yao, 2011):

$$E_c = \int_{t_0}^{t_1} p_p(t) q_p(t) dt = \int_{t_0}^{t_1} n_p p_p(t) V_p(t) dt, \quad (42)$$

$$\eta_e = \frac{\int_{t_0}^{t_1} v_c(t) [p_1(t) A_1 - p_2(t) A_2] dt}{\int_{t_0}^{t_1} n_p p_p(t) V_p(t) dt}. \quad (43)$$

In contrast to the traditional controller, the efficiency improvement η_i of the proposed controller can be expressed as

$$\eta_i = \eta_{ep} - \eta_{et}, \quad (44)$$

where η_{ep} denotes the energy efficiency of the proposed controller or the maximum controller, and η_{et} the energy efficiency of the traditional controller. In the traditional controller, the valve control signal directly follows the signal of the input device (e.g., joysticks) by the operators. In this way, the operator is able to obtain the best controllability of the mobile machinery. Therefore, the velocity of the traditional controller is considered as the desired velocity. The root-mean-square (RMS) error is used to evaluate the velocity performance of the proposed controller and the maximum controller, which is expressed as

$$I_v = \sqrt{\frac{\int_{t_0}^{t_1} [v(t) - v_c(t)]^2 dt}{t_1 - t_0}}, \quad (45)$$

where $v(t)$ is the velocity of the proposed controller or the maximum controller. The energy efficiencies and the velocity errors are shown in Table 3. It can be seen from Table 3 that the maximum controller achieves better efficiency performance, but its velocity error is larger than that of the proposed controller.

Table 3 Performance comparison of the three controllers under the constant input commands

Controller	E_c (J)	η_e (%)	η_i (%)	I_v (m/s)
Traditional	5152	39.50	—	—
Proposed	4742	46.30	6.80	0.0040
Maximum	4610	52.60	13.10	0.0156

Then, tests under switched input commands were carried out. The control signals and the driving forces of the proposed controller are shown in Fig. 11. The arm cylinder retracts first and then extends. The input device delivers the 4.5 V signal to the valve in 10–17 s. Then the control signal linearly increases to 7.7 V in 17–17.5 s, and finally it maintains at 7.7 V in 17.5–22.5 s. It is found that the valve signal generated by the proposed controller is adaptively regulated based on the driving force shown in Fig. 11b.

The comparison among the load velocities is shown in Fig. 12. The load velocity of the traditional controller is consistent with that of the proposed controller. The hydraulic cylinder with the maximum controller makes an overspeed movement (see the velocity after 18 s in Fig. 12) when it is exerted by an overrunning load. The system pressure characteristics are shown in Fig. 13. The system pressure of the proposed controller is reduced in the cylinder retracting process and it is almost the same with the traditional controller in the cylinder extending process. The energy performance and the velocity errors are listed in Table 4. Similarly, it is seen that although the proposed controller obtains a smaller efficiency improvement than the maximum controller, its velocity is more consistent with that of the traditional controller.

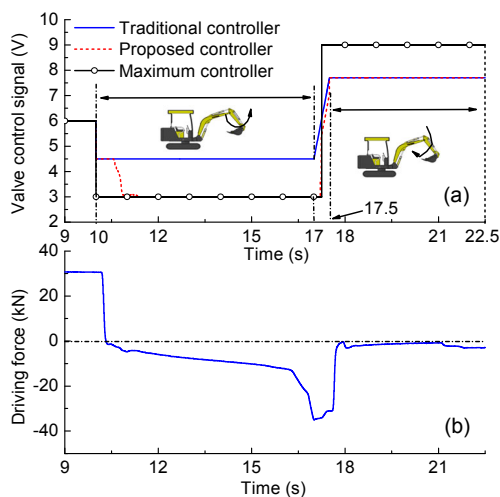


Fig. 11 Comparison of the valve control signals (a) and the driving force (b) under the switched input commands

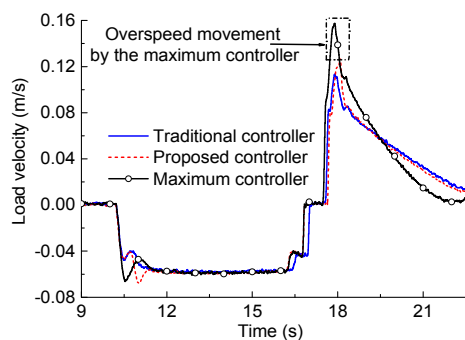


Fig. 12 Load velocity comparison under the switched input commands

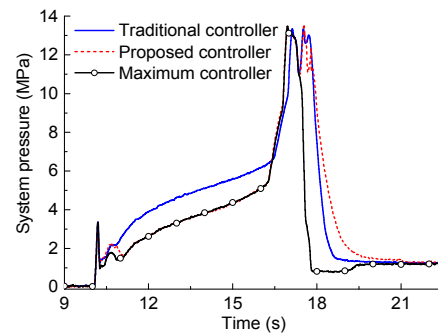


Fig. 13 System pressure comparison under the switched input commands

Table 4 Performance comparison of the three controllers under the switched input commands

Controller	E_c (J)	η_e (%)	η_i (%)	I_v (m/s)
Traditional	10580	22.0	—	—
Proposed	8724	25.2	3.2	0.0063
Maximum	7892	29.1	7.1	0.0145

The results above indicate that the energy efficiency can be improved by the proposed controller or the maximum controller. More importantly, the velocity performance of the proposed controller basically coincides with that of the traditional controller. Only depending on the load force in overrunning load conditions, the cylinder velocity cannot be regulated in an expected manner by the maximum controller, although higher energy efficiency can be achieved.

5 Conclusions

In this paper, an electronic valve control method is proposed to improve the controllability of the energy-saving electrohydraulic system for mobile machinery. Combined with the electrohydraulic flow matching concept, a compensation controller is proposed to reduce the pressure drop over the control valve, consisting of a static compensator and a differential dynamic compensator. At the same time, the velocity performance of the proposed controller can be ensured under the overall working conditions. Tests on a test rig with a hydraulic excavator were carried out. The results indicated that the energy efficiencies under constant and switched input commands were reduced respectively by 6.8% and 3.2%

with the proposed controller, while the velocity control performance was consistent with that of the traditional controller.

Future work will be focused on testing the effectiveness of the proposed controller in actual digging cycles. In addition, new controllers in multi-actuator systems will be developed to further improve the energy efficiency and ensure the dynamic control performance.

References

- Axin, M., 2013. Fluid Power Systems for Mobile Applications: with a Focus on Energy Efficiency and Dynamic Characteristics. Licentiate Thesis, Linköping University, Linköping, Sweden.
- Axin, M., Eriksson, B., Krus, P., 2014. Flow versus pressure control of pumps in mobile hydraulic systems. *Proceedings of the Institution of Mechanical Engineers, Part I: Journal of Systems and Control Engineering*, **228**(4): 245-256.
<http://dx.doi.org/10.1177/0959651813512820>
- Borghi, M., Zardin, B., Pintore, F., et al., 2014. Energy savings in the hydraulic circuit of agricultural tractors. *Energy Procedia*, **45**:352-361.
<http://dx.doi.org/10.1016/j.egypro.2014.01.038>
- Cristofori, D., Vacca, A., Ariyur, K., 2012. A novel pressure-feedback based adaptive control method to damp instabilities in hydraulic machines. *SAE International Journal on Commercial Vehicles*, **5**(2):586-596.
<http://dx.doi.org/10.4271/2012-01-2035>
- Daher, N., Ivantysynova, M., 2015. Yaw stability control of articulated frame off-highway vehicles via displacement controlled steer-by-wire. *Control Engineering Practice*, **45**:46-53.
<http://dx.doi.org/10.1016/j.conengprac.2015.08.011>
- DeBoer, C.C., Yao, B., 2001. Velocity control of hydraulic cylinders with only pressure feedback. Proceedings of ASME International Mechanical Engineering Congress and Exposition.
- Du, C., Plummer, A., Johnston, N., 2016. Performance analysis of an energy-efficient variable supply pressure electro-hydraulic motion control system. *Control Engineering Practice*, **48**:10-21.
<http://dx.doi.org/10.1016/j.conengprac.2015.12.013>
- Ekoru, J.E., Pedro, J.O., 2013. Proportional-integral-derivative control of nonlinear half-car electro-hydraulic suspension systems. *Journal of Zhejiang University-SCIENCE A (Applied Physics & Engineering)*, **14**(6):401-416.
<http://dx.doi.org/10.1631/jzus.A1200161>
- Finkel, R., Helduser, S., 2008. Energy-efficient electro-hydraulic control systems for mobile machinery/flow matching. Proceedings of the 6th International Fluid Power Conference.
- Garimella, P., Yao, B., 2002. Nonlinear adaptive robust observer for velocity estimation of hydraulic cylinders using pressure measurement only. Proceedings of ASME International Mechanical Engineering Congress and Exposition.
- Heikkilä, M., Linjama, M., 2013. Displacement control of a mobile crane using a digital hydraulic power management system. *Mechatronics*, **23**(4):452-461.
<http://dx.doi.org/10.1016/j.mechatronics.2013.03.009>
- Heybroek, K., 2008. Saving Energy in Mobile Machinery Using Displacement Control Hydraulics: Concept Realization and Validation. PhD Thesis, Linköping University, Linköping, Sweden.
- Inderelst, M., Sgro, S., Murrenhoff, H., 2010. Energy recuperation in working hydraulics of excavators. The Bath/ASME Symposium on Fluid Power and Motion Control.
- Ketonen, M., Linjama, M., Huhtala, K., 2010. Retrofitting digital hydraulics—an analytical study. Proceedings of the 9th International Fluid Power Conference.
- Kim, D., Son, D.H., Jeon, D., 2012. Feed-system autotuning of a CNC machining center: rapid system identification and fine gain tuning based on optimal search. *Precision Engineering*, **36**(2):339-348.
<http://dx.doi.org/10.1016/j.precisioneng.2011.09.007>
- Kogler, H., Scheidl, R., 2008. Two basic concepts of hydraulic switching converters. Proceedings of the 1st Workshop on Digital Fluid Power.
- Laamanen, M.S.A., Vilenius, M., 2003. Is it time for digital hydraulics? Proceedings of the 8th Scandinavian International Conference on Fluid Power.
- Lin, X., Pan, S., Wang, D., 2008. Dynamic simulation and optimal control strategy for a parallel hybrid hydraulic excavator. *Journal of Zhejiang University-SCIENCE A*, **9**(5):624-632.
<http://dx.doi.org/10.1631/jzus.A071552>
- Linjama, M., 2011. Digital fluid power: state of the art. Proceedings of the 12th Scandinavian International Conference on Fluid Power.
- Liu, W., 2011. Investigation into the Characteristics of Electrohydraulic Flow Matching Control Systems for Excavators. PhD Thesis, Zhejiang University, Hangzhou, China (in Chinese).
- Merrill, K.J., Holland, M.A., Lumkes, J.H., 2010. Efficiency analysis of a digital pump/motor as compared to a valve plate design. Proceedings of the 7th International Fluid Power Conference.
- Mettälä, K., Djurovic, M., Keuper, G., et al., 2007. Intelligent oil flow management with EFM: the potentials of electrohydraulic flow matching in tractor hydraulics. Proceedings of the 10th Scandinavian International Conference on Fluid Power, p.25-34.
- Minav, T.A., Laurila, L.I.E., Pyrhönen, J.J., 2013. Design and

- control of a closed-loop hydraulic energy-regenerative system. *Automation in Construction*, **30**:144-150.
<http://dx.doi.org/10.1016/j.autcon.2012.11.009>
- Stelson, K.A., 2011. Saving the world's energy with fluid power. Proceedings of the 8th JFPS Intentional Symposium on Fluid Power.
- Troxel, N.A., Yao, B., 2011. Hydraulic cylinder velocity control with energy recovery: a comparative simulation study. Proceedings of the ASME 2011 Dynamic Systems and Control Conference.
- Wang, T., Wang, Q., 2014. An energy-saving pressure-compensated hydraulic system with electrical approach. *IEEE/ASME Transaction on Mechatronics*, **19**(2):570-578.
<http://dx.doi.org/10.1109/TMECH.2013.2250296>
- Xu, B., Cheng, M., Yang, H., et al., 2015a. A hybrid displacement/pressure control scheme for an electrohydraulic flow matching system. *IEEE/ASME Transaction on Mechatronics*, **20**(6):2771-2782.
<http://dx.doi.org/10.1109/TMECH.2015.2411315>
- Xu, B., Sun, Y.H., Zhang, J.H., et al., 2015b. A new design method for the transition region of the valve plate for an axial piston pump. *Journal of Zhejiang University-SCIENCE A (Applied Physics & Engineering)*, **16**(3):229-240.
<http://dx.doi.org/10.1631/jzus.A1400266>
- Xu, B., Ding, R.Q., Zhang, J.H., et al., 2015c. Pump/valves coordinate control of the independent metering system for mobile machinery. *Automation in Construction*, **57**:98-111.
<http://dx.doi.org/10.1016/j.autcon.2015.04.012>
- Xu, B., Hu, M., Zhang, J.H., et al., 2016. Characteristics of volumetric losses and efficiency of axial piston pump with respect to displacement conditions. *Journal of Zhejiang University-SCIENCE A (Applied Physics & Engineering)*, **17**(3):186-201.
<http://dx.doi.org/10.1631/jzus.1500197>
- Yang, H.Y., Pan, M., 2015. Engineering research in fluid power: a review. *Journal of Zhejiang University-SCIENCE A (Applied Physics & Engineering)*, **16**(6):427-442.
<http://dx.doi.org/10.1631/jzus.A1500042>
- Zaev, E., Rath, G., Kargl, H., et al., 2013. Energy efficient active vibration damping. Proceedings of the 13th Scandinavian International Conference on Fluid Power.

中文概要

题目：基于阀补偿的电液流量匹配节能系统的动态性能改进

目的：电液流量匹配系统通过前馈指令信号来调节泵排量，故可采用增大阀口开度的方法来降低能量损失，但是该方法降低了超越负载工况下的操控性能。为改进该工况下的系统动态性能，本文旨在研究电液流量匹配系统泵阀控制方法，在提高系统效率的前提下，提高系统动态性能。

创新点：提出了基于比例阀补偿的动态性能改进方法，研制了考虑动静态性能补偿的比例阀控制器，提高了系统速度控制性能。

方法：1. 建立电液流量匹配节能系统数学模型，分析在超越或阻抗工况下的系统速度控制需求；2. 提出基于比例阀开口补偿的控制方法（图 2）以提高系统动态性能；3. 相对于传统阀口控制方法，分析提出的方法在不同负载工况下的节能特性；4. 通过频域分析法研究系统稳定性，并提出保证系统稳定和动态性能的参数选取准则。

结论：1. 相比传统阀口控制方法，提出的基于比例阀补偿的控制方法能够提高 3.2%~6.8% 的系统效率；2. 相对于阀口全开控制方法，所提方法的优势在于能保证系统在不同工况下的动态控制性能，尤其能保证在超越负载工况下的系统可控性；3. 所提方法不仅提高了设备的效率，也保证了系统的操控性能。

关键词：补偿控制；节能；流量匹配；移动机械